Structured-light three-dimensional scanning for process monitoring and quality control in precast concrete production

Rongxuan Wang, Yinan Wang, Sonam Devadiga, Isaac Perkins, Zhenyu (James) Kong, Xiaowei Yue

- This paper presents the use of a structured-light three-dimensional scanner to allow for efficient and real-time inspections of precast concrete specimens. This proposed quality assurance system reviews the quality of a product in three key features: overall dimensions, embedded locations, and surface finishes.
- The experimental program demonstrated that the proposed quality assurance system can quantitatively measure the surface finish of a precast concrete object, recognize and check the location of the embedded metal parts, and validate the overall geometry with the design.

PCI Journal (ISSN 0887-9672) V. 66, No. 6, November–December 2021.
PCI Journal is published bimonthly by the Precast/Prestressed Concrete Institute, 8770 W. Bryn Mawr Ave., Suite 1150, Chicago, IL 60631.

Quality control is a crucial step in the fabrication of precast concrete products. In addition to each component's mechanical properties, three key features ensure a high-quality product: overall dimensions, embedded part locations, and surface finishes. Measuring these three quality features in a highly repeatable and efficient way is challenging. Currently, operators use tape measures to obtain critical overall dimensions and embedded part locations. The tape measure can provide quantitative measurements, but it is not accurate and efficient enough. Measurements from different operators may deviate, and other factors may also affect measurement precision. For example, working temperature can be a source of measurement error because the tape measure, depending on the material, may stretch in high temperatures or shrink in low temperatures. Furthermore, using a tape measure may pose a safety risk if an operator is required to climb onto a ladder or the precast concrete specimen itself multiple times to acquire all of the critical dimensions. As for the third key quality feature, the level of surface finish, judging this relies on the workers' experience because of limited options in real-time measurement devices. Such an experience-based quality control method may result in product quality inconsistency and lead to customer dissatisfaction. Innovative measurement and quality control methods are needed.

In recent years, researchers have developed several quality inspection methods based on the applications of three-dimensional (3-D) scanning and point cloud data.[1] Depending on the specific tasks, the existing conventional methods

focus on dimensional quality inspection, surface quality inspection, or displacement inspection. For dimensional quality inspection, Kim et al.[2] proposed an automated and noncontact measurement technique using a terrestrial laser scanner to measure and assess the dimensions of precast concrete panels. Wang et al.[3] extended the study from checking the dimensional quality of regular shapes to checking shapes with geometric irregularities. Kim and associates[4] improved the dimensional quality inspection technique by using principal component analysis and testing its performance on full-scale precast concrete objects.

Research on surface quality inspection has mainly targeted surface defects. Liu et al.[5] employed a digital image processing technique to assess concrete cracks. Kim et al.[6] presented a technique that can simultaneously localize and quantify spalling defects on concrete surfaces. Wang et al.[7] used laser scanning to conduct surface flatness and distortion inspection of precast concrete elements.

Recent studies on displacement inspection have explored techniques to detect displacement in large-scale concrete pieces. Gonzalez-Aguilera et al.[8] proposed a statistical method to monitor the static and dynamic behaviors of large dams based on 3-D laser scanning. Riveiro et al.[9] developed a terrestrial-laser-scanner- and photogrammetry-based methodology for bridge minimum vertical clearance and overall geometry inspections. Oskouie et al.[10] extracted geometric features of highway retaining walls from laser-scan data and analyzed them to detect displacements.

There are two limitations in the aforementioned studies. First, the point cloud data were acquired using a time-of-flight laser scanner.[11] This type of machine shoots a laser beam onto the surface and determines the distance between the machine and the surface by calculating the laser travel time. Although this method is accurate and has long-range coverage, it is time-consuming when high-density surface data are required because it only measures one spot each time.

Photogrammetry[12] is one alternative 3-D scanning technique. It uses multiple pictures taken from different angles to complete the 3-D reconstruction. This method has the advantage of low cost because only one camera is needed, but it has low accuracy.

Another option is to use structured-light scanning (SLS)[13], which uses a triangulation-based method. This type of 3-D scanner consists of two cameras and a projector. The projector projects a fringe pattern onto the surface, and from the camera's point of view, the pattern is distorted. Such distortion can be used to calculate the surface geometry. SLS has three advantages compared with laser scanning. First, it does not create any laser safety hazards, such as eye injury, and provides a safer working environment in which no extra eye protection is required. Second, SLS is faster than laser scanning and yields higher-resolution results. An SLS scanner takes just a few seconds to scan millions of data points, whereas a laser scanner scans line by line and at a slower pace. Third, SLS costs less to purchase (typically just a few thousand dollars, whereas a laser scanner can cost more than $20,000). SLS also works well in a range of light conditions because the scanning software can automatically optimize the settings of the camera (exposure time and gain) and projector (brightness). One potential concern is that the coverage area of the projector that comes with commercialized SLS systems may be too small for scanning typical full-scale precast concrete parts (such as those longer than 20 m [66 ft]). This issue can be resolved by replacing the current office-grade projector with a professional-grade projector (about $2000 to $3000), which can provide a very large coverage area. Suggestions for implementing SLS systems in a factory environment are provided at the end of this paper.

The second limitation of the previously described research is that the studies all mainly focused on inspecting a single type of quality issue in precast concrete. However, on the real production line, a systematic quality inspection including the surface finish check, overall dimension check, and embedded parts location check is needed before the final product can be delivered. Furthermore, precasters need user-friendly, operator-accessible software to integrate all the developed techniques.

The main purpose of this paper is to propose a 3-D scanning-based quality inspection and data analytics system for precast, prestressed concrete production. The specific innovations can be summarized as follows:

- adapting SLS to perform the surface and geometric measurements
- developing a set of algorithms to conduct a systematic quality inspection of precast concrete
- providing a user-friendly graphical user interface (GUI) to standardize and simplify the operations

The framework of the proposed quality control system (**Fig. 1**) contains a set of hardware and algorithms and provides a highly reliable and repeatable way to accurately and efficiently complete the three key quality inspection tasks (surface finish check, overall dimension check, and embedded parts location check). This system can substantially reduce operator errors and safety hazards and has the advantages of low cost and short measuring time. When this system was tested using a precast concrete sample that contained multiple surface finishes, complicated surface geometries, and embedded metal plates to mimic all three critical features in real concrete products (**Fig. 2**), it proved to be effective.

Experiment setup and raw data visualization

In the experiment, a mock-up concrete sample with complex shapes, embedded metal parts, and multiple types of surface finish was made by Tindall Corp. The computer-aided design (CAD) drawing of the precast concrete sample is shown in

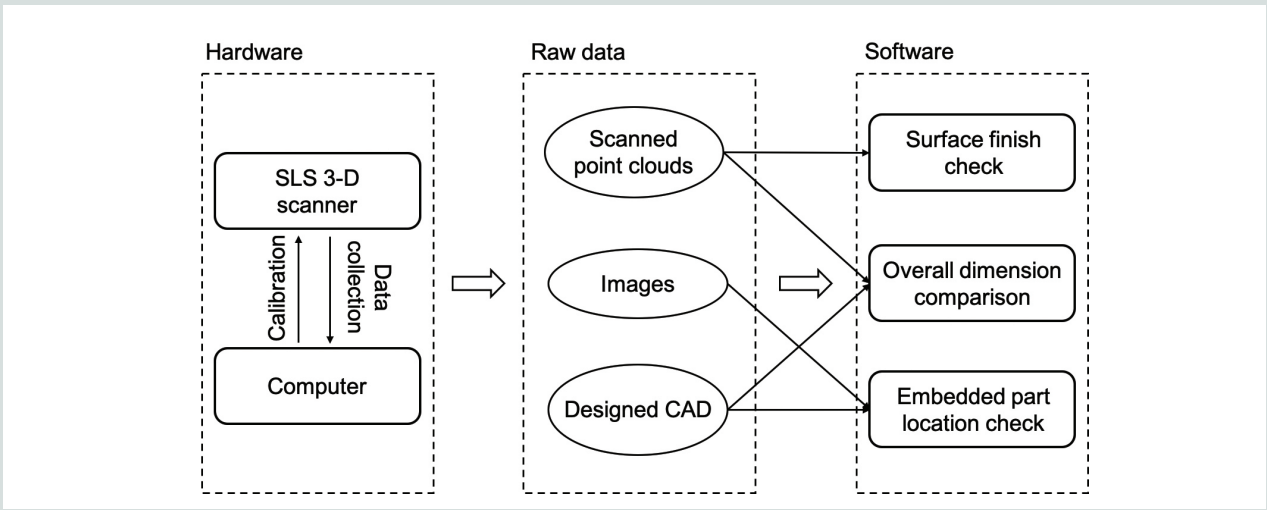

Figure 1. The framework of the proposed quality control system. Note: CAD = computer-aided design; SLS = structured-light scanning; 3-D = three-dimensional.

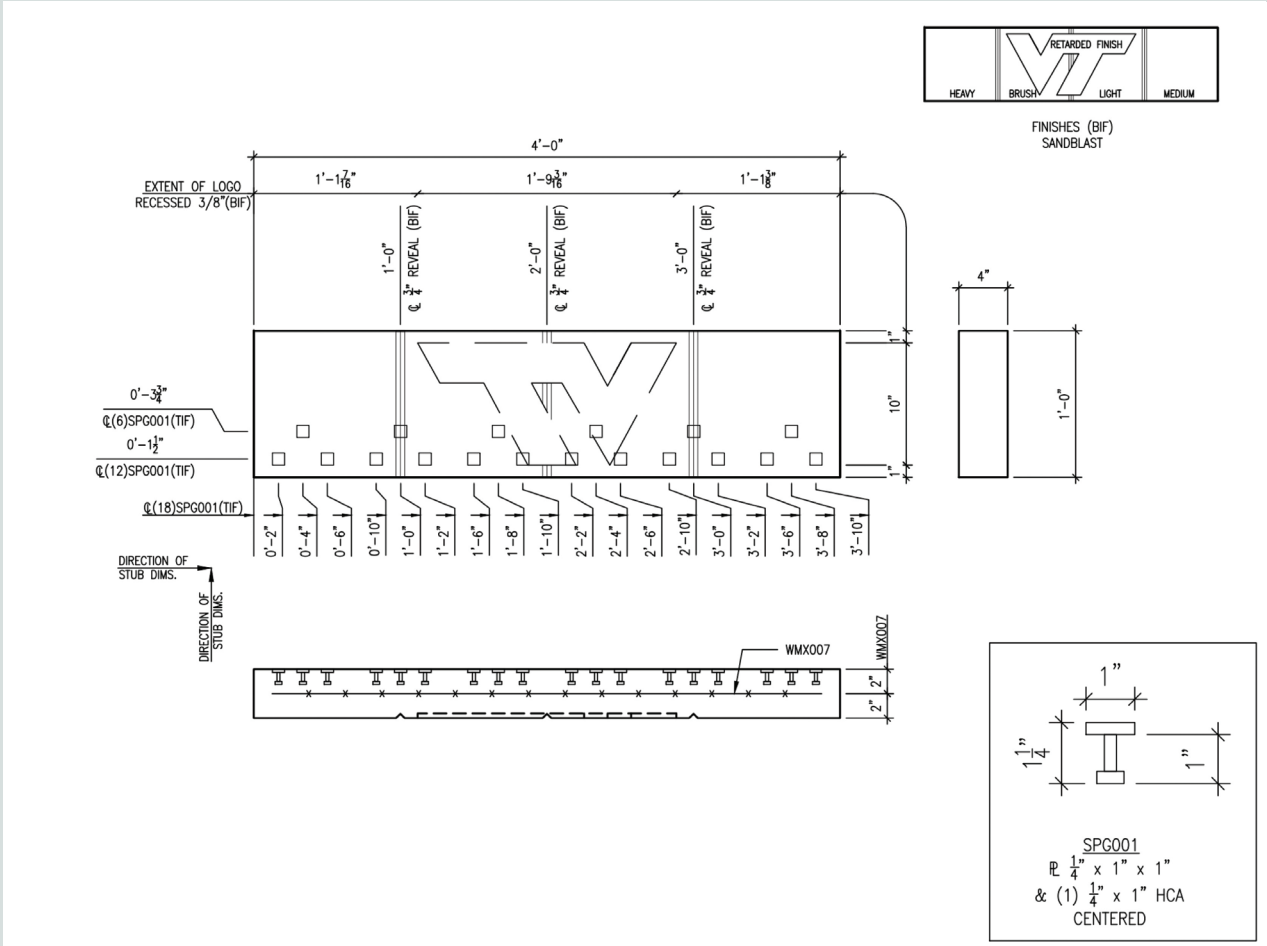

Figure 2. Engineering drawing for mock-up part. Note: BIF = bottom in form; CL = center line; Dims. = dimension; HCA = headed concrete anchor; PL = plate; SPG001 = part number of the anchor; TIF = top in form; WMX007 = part number of the reinforcing bar. 1" = 1 in. = 25.4 mm; 1' = 1 ft = 0.305 m; 1 lb = 4.448 N; 1 psi = 6.895 kPa.

Fig. 2. This test specimen is 4 ft (1.2 m) long, 1 ft (0.3 m) wide, and 4 in. (102 mm) thick. It is a scaled-down test sample that has all the features of interest in real practice. For example, as Fig. 2 illustrates, five commonly used surface finishes are applied to the different regions of the sample surface to test the capability of the proposed system.

A 3-D scanner was used to capture the surface point cloud data from the mock-up sample. **Figure 3** shows the experimental setup. The precast concrete sample was lifted by a crane, and the scanner was placed about 5 ft (1.5 m) away from the sample. Each of the front and back surfaces was covered by two separate scans. The scanner further registered and fused the two front and two back scans to generate the complete surfaces. The first and second rows in **Fig. 4** present the scanned data with and without surface texture information, respectively. Each scan took about 3 seconds to capture the raw data and 15 seconds for the software to complete the triangulation calculation. Once the scan was finished, the result could be loaded into the GUI for quality analysis.

Functional modules

The software for the proposed quality assurance system consists of three modules: overall dimension check, embedded part location check, and surface finish check. The detailed methodologies for these three functional modules are discussed in this section.

Overall dimension check

The overall dimension check evaluates whether the sample's overall geometry satisfies the geometric dimensions and tolerances specified in the design. This check can identify the areas that failed to meet the designed shape and tolerances. Current quality assurance procedures are achieved by limited point-to-point measurements, such as using a tape measure to measure the length of a precast concrete component; however, precast concrete can distort during curing, which creates a 3-D shape change that cannot be measured accurately with a tape measure. With the proposed quality assurance system, a comparison between the entire surface and the designed geometry is conducted after the concrete is fully cured and cooled. To do so, the CAD model (Fig. 4) is first obtained based on the engineering design (Fig. 2). **Figure 5** illustrates the three-step process of overall dimension check:

1. Register the iterative closest point (ICP) between the designed point cloud from the CAD model and scanned point cloud data.

2. Calculate the pointwise distance based on registration results.

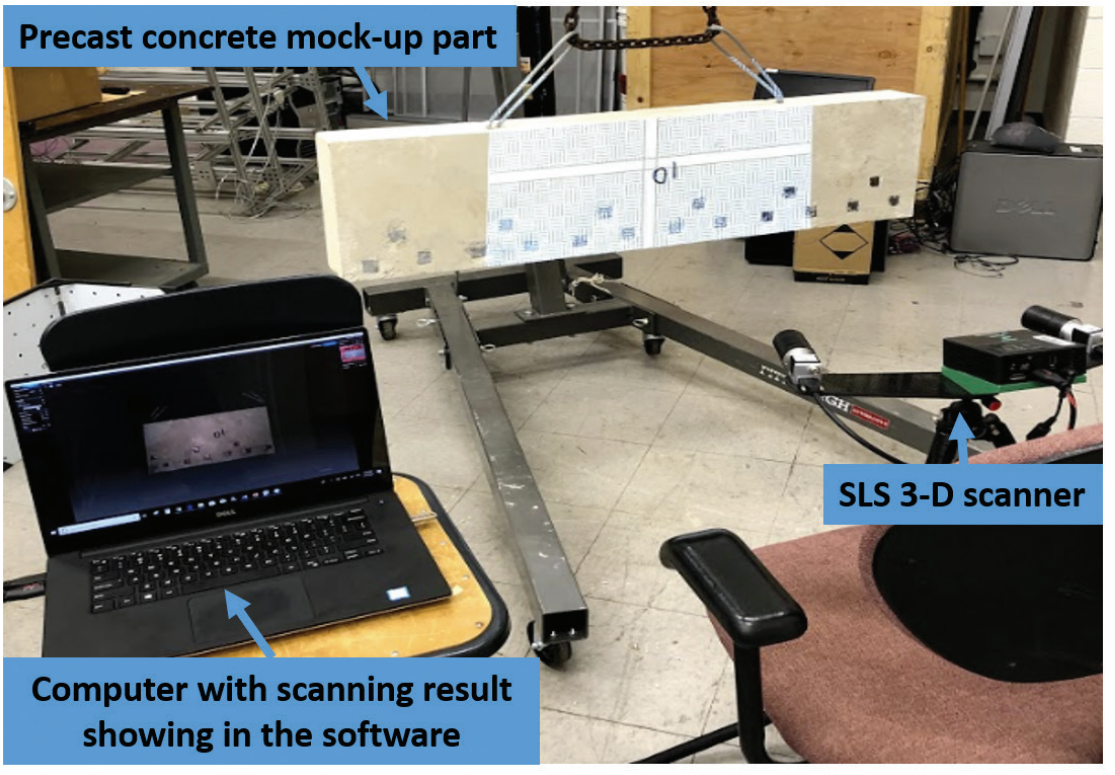

Figure 3. Three-dimensional scanning process of precast concrete sample. Note: SLS = structured-light scanning.

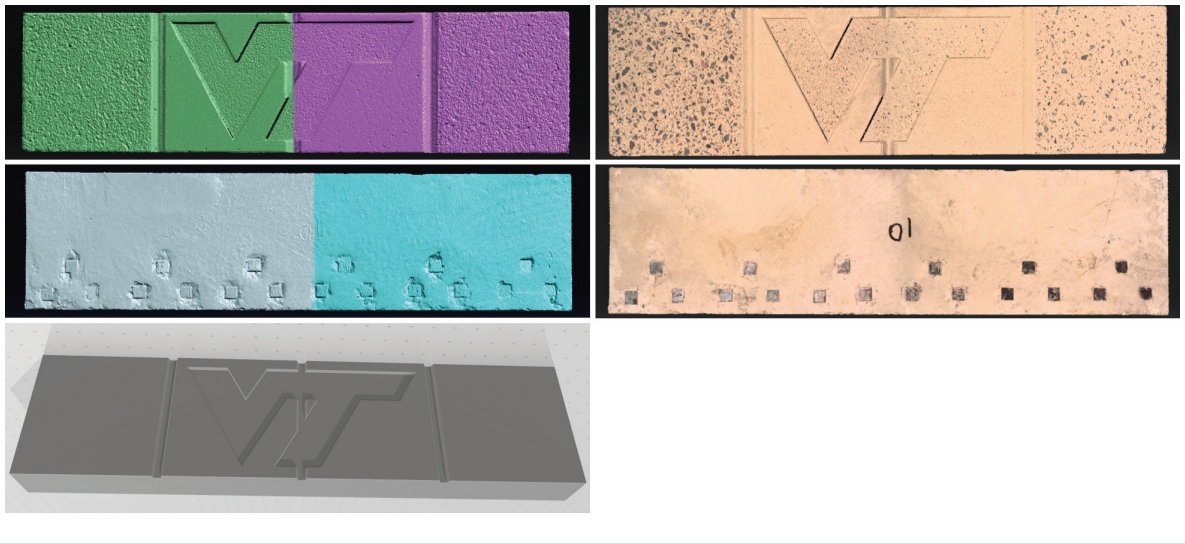

Figure 4. The top row shows three-dimensional surface scan results without texture information and with different colors to represent the results from different scans. The second row shows three-dimensional surface scan results with texture information. The third row shows the computer-aided design model of the mock-up part.

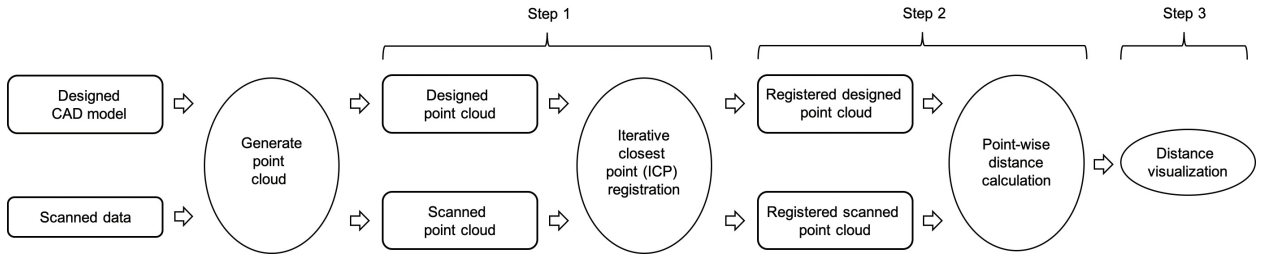

Figure 5. Process of overall dimension check. Note: CAD = computer-aided design.

3. Visualize the distance to show the difference between the designed product and the real product.

Registration matches two point clouds for the same object by rotation and translation. In this experiment (Fig. 5), the designed point cloud was sampled from the CAD model to represent the standard geometry of the precast concrete component and the SLS 3-D scanner was used to collect the scanned point cloud representing the actual dimensions of the product. Ideally, after registration, these two point clouds would be perfectly matched; this would mean there are no production errors and the product is strictly consistent with the design; however, production errors are inevitable and will lead to deviations in some local areas.

The ICP algorithm has been used to minimize the position difference between two point clouds.[14] If the designed point cloud C is denoted as $C \in \mathbb{R}^{N\times 3}$ and the scanned point cloud S is denoted as $S \in \mathbb{R}^{N\times 3}$, where N is the number of points, the objective function of registration can be formulated as follows.

$$\min\left(dist\left(\tilde{S},C\right)\right)$$

subject to $\tilde{S} = R \times S + T$

where

min = minimum

$dist(.)$ = distance function evaluating the difference between two point clouds

$\tilde{S}$ = registered scanned point cloud

R = rotation matrix

T = translation matrix

Algorithm 1, the iterative closest point algorithm, summarizes the ICP algorithm procedure. After ICP registration, the registered scanned point cloud $\tilde{S}$ is generated and then the deviation between the $\tilde{S}$ and C is calculated using the multiscale model–to–model cloud comparison (M3C2) distance[15] to reflect the production error.

For algorithm 1, input the following:

1. $C \in \mathbb{R}^{N\times 3}$, $S \in \mathbb{R}^{N\times 3}$
2. initial estimate of correspondence points in C and S

Then loop the following:

3. **While not** Converge **Do**.
4. Determine the correspondence: for each point in S, find the closest point in C.
5. Find the best transform (rotation and translation matrices) for this correspondence.
6. Transform S.

Embedded part location check

If the metal embedded plates used to attach precast concrete parts are mispositioned during the manufacturing process, the product cannot be installed properly. To address this quality concern, the embedded part location check was developed to obtain the positions of embedded metal parts and then compare those positions with positions in the design file. In the experiment, multiple metal plates were embedded on the surface of the precast concrete sample (Fig. 2). **Figure 6** illustrates the process of metal plate detection and comparison. The inputs of the embedded part location check are raw images taken during the 3-D scanning process. The detection process has five steps:

1. image binarization
2. noise filtering
3. edge detection
4. shape detection
5. and position extraction and comparison

This algorithm is not limited to detecting metal plates; it can also be easily extended to detect other critical parts, such as hooks or slots.

Image binarization

We binarize the original image and transform it into black and white to improve efficiency without using losing critical information. Note that the original image from the experiment is in RGB color format and can be denoted as $I \in \mathbb{R}^{H\times W\times 3}$, where I is a three-way tensor representing the color image and H and W represent the height and width of the image, respectively. The intensity of each pixel I_{ij} is represented by a vector [r, g, b], which denotes the intensity of the colors red, green, and blue in this pixel. Before binarization, the image is initially transformed into grayscale using the equation given below.

$$\tilde{I}_{i,j} = 0.3\times I_{i,j}(1) + 0.59\times I_{i,j}(2) + 0.11\times I_{i,j}(3)$$

where

$\tilde{I}$ = the grayscale image with the shape of $H \times W$

$\tilde{I}_{i,j}$ = the grayscale pixel intensity at position (i,j) in grayscale image

$I_{i,j}(1)$ = the intensity of color red

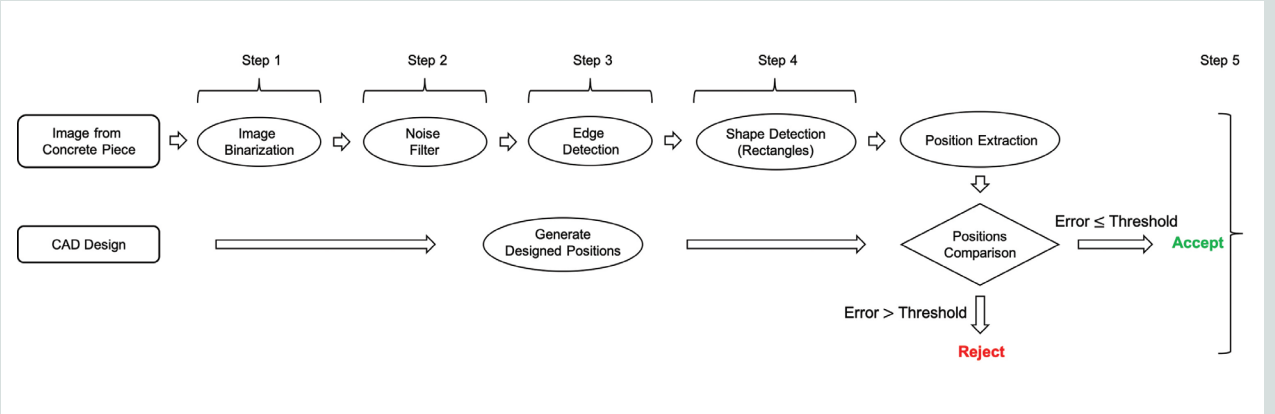

Figure 6. Process of metals detection and comparison. Note: CAD = computer-aided design.

$I_{i,j}(2)$ = the intensity of color green

$I_{i,j}(3)$ = the intensity of color blue

The binarization is then conducted on the grayscale image by setting a threshold value to binarize the value of each pixel. For a given threshold value, if the pixel value in the grayscale image is greater than the threshold, the corresponding pixel value in the binarized image is set to 255 (white), otherwise the corresponding pixel value is set to 0 (black).

Noise filtering

Some noise (black dots) might remain in the binarized image because the concrete might not be perfectly clean and smooth. The second step is to filter the noise to make the background as smooth as possible. The median filter is selected to eliminate noise from the background. The aim is to slide a square window over the image and replace the center pixel value with the median of all pixel values in the window (5 × 5 pixels).

Edge detection

After noise filtering, the edges of embedded parts can be detected by transforming the image to a gradient map and then using high-pass filters to capture the positions where pixel values change significantly (from white to black). The gradient operator is applied to the noise-filtered image to calculate the magnitude of the pixel-wise gradient. The expressions of a typical gradient operator are as follows.

$$\frac{\partial \tilde{I}_{i,j}}{\partial x} = -\frac{1}{2}\tilde{I}_{i-1,j} + \frac{1}{2}\tilde{I}_{i+1,j}$$

$$\frac{\partial \tilde{I}_{i,j}}{\partial y} = -\frac{1}{2}\tilde{I}_{i,j-1} + \frac{1}{2}\tilde{I}_{i,j+1}$$

$$\left|\nabla \tilde{I}\right| = \sqrt{\frac{\partial \tilde{I}^2}{\partial x} + \frac{\partial \tilde{I}^2}{\partial y}}$$

where

$\tilde{I}_{i-1,j}$ = the intensity of pixel at position $(i-1,j)$ in grayscale image $\tilde{I} \in \mathbb{R}^{H \times W}$

$\tilde{I}_{i+1,j}$ = the intensity of pixel at position $(i+1,j)$ in grayscale image $\tilde{I} \in \mathbb{R}^{H \times W}$

$\tilde{I}_{i,j-1}$ = the intensity of pixel at position $(i,j-1)$ in grayscale image $\tilde{I} \in \mathbb{R}^{H \times W}$

$\tilde{I}_{i+1,j}$ = the intensity of pixel at position $(i,j+1)$ in grayscale image $\tilde{I} \in \mathbb{R}^{H \times W}$

After determining the magnitude of the pixel-wise gradient, a gradient threshold is applied to decide whether edges are present at an image point.

Shape detection

In many cases, workers use pens to mark part numbers on precast concrete components, as seen as "01" in the scans. These marks cannot be easily removed from images and would be counted as edges in the previous edge-detection step. Therefore, to address this type of image noise, we apply a shape detection method.[16] During shape detection, connected edges are assigned to the same contour, and then the shapes of all of the generated contours are checked. Only contours with the rectangular shape are preserved in the image, allowing the rectangular embedded parts to be successfully identified.

Position extraction and comparison

The locations of the detected embedded parts can be found by the centers of the rectangular contours. These locations are recorded in pixels. Subsequently, the pixel-to-dimension ratio of the image is calculated based on the corresponding concrete dimensions to transform the metal plate positions from pixels to inches.

After extracting the positions of embedded parts, position errors can be calculated and annotated by comparing the extracted positions with the designed positions in the CAD file. As the sizes of metal parts are determined, a position error is defined as the distance between the center of an extracted location and the center of the corresponding designed location. The error is calculated by the Euclidean distance between the designed center position (x,y) and the product's center position $(\hat{x},\hat{y})$, which is given as follows:

$$\text{error} = \sqrt{(x-\hat{x})^2 + (y-\hat{y})^2}$$

Surface finish check

The surface finish check aims to provide quantitative guidance for architectural precast concrete finishers to meet the requirements of their customers. The surface finishes are calculated based on the point cloud data acquired from the 3-D scanner and can be quantified by the mean distance between the measured points and the locally fitted plane. The globally fitted plane is not used here because the real product might have deformations due to stress or molding error. These deformations introduce errors in surface finish calculations. Calculating the surface finish based on the locally fitted plane can eliminate the influence of overall deformation.

Calculating distances between point cloud and fitted plane

The surface point cloud data can be represented in the 3-D space by a set of points (x_i,y_i,z_i) that represent the position of point i along each axis. To generate a locally fitted plane, the first step is to segment a subregion of the point clouds. Second, we suppose that the selected points distribute on the same plane, with the expression of the plane given as Eq. (1).

$$A\beta = B \quad (1)$$

where

A $= \begin{pmatrix} x_1 & y_1 & 1 \\ \vdots & \vdots & \vdots \\ x_N & y_N & 1 \end{pmatrix}$, represented by $A \in \mathbb{R}^{N\times 3}$, the i_{th} row of A is denoted as $A_i = [x_i, y_i, 1]$

β = unknown parameters of this plane, represented by $\beta \in \mathbb{R}^{3\times 1}$

B = $[z_1,\ldots,z_N]^T$, represented by $B \in \mathbb{R}^{N\times 1}$, the i_{th} row of B is denoted as $B_i = [z_i]$

Given the points in the segmented subregion, we can derive the solution of unknown parameters (Eq. [2]).

$$\hat{\beta} = (A^T A)^{(-1)} A^T B \quad (2)$$

$\hat{\beta}$ = the estimated parameters of this plane

A^T = the transpose of A

The absolute distance D between the selected points and the locally fitted plane can be calculated by Eq. (3).

$$D = \left| B - A\hat{\beta} \right| \quad (3)$$

where

$D \in \mathbb{R}^{N\times 1}$

|.| = the element-wise absolute operation

The positive values in $B - A\hat{\beta}$ represent the corresponding points above the fitted plane, and the negative values represent the corresponding points below the fitted plane.

The mean and variance of D are selected to represent the roughness of the segmented subregions. The second row in **Fig. 7** presents some examples of the surface finish visualization.

Summarizing local results to reflect overall surface finish

Given D is calculated for each subregion, the overall surface finish can be represented by the mean and variance of D from all subregions. The test sample had five different surface finishes: light, medium, heavy, brush, and retarded (Fig. 2). Each finish was quantified individually. Figure 7 shows the pipeline to obtain the surface finish statistics for the test sample. The entire process can be summarized in three steps. First, for each

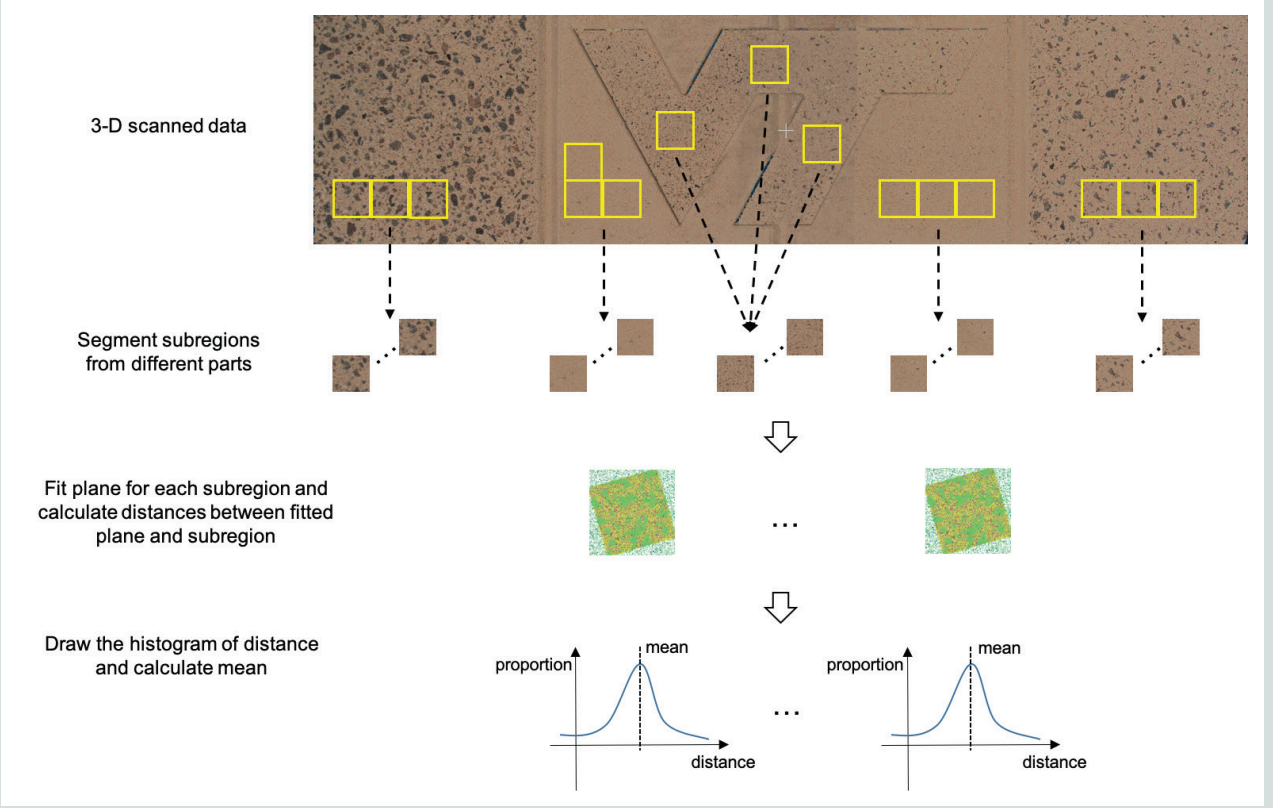

Figure 7. Overview of the surface finish statistics pipeline. Note: 3-D = three-dimensional.

type of finish, 20 subregions (each approximately 1.2 × 1.2 in. [30 × 30 mm]) were segmented from the raw data. Then, for each subregion, the pointwise distance between the subregion and its fitted plane was calculated based on Eq. (1) through (3). Finally, for each type of finish, the roughness statistics were calculated using all the corresponding segmented subregions. The control limit was set to 1 standard deviation.

Experiment results

This section describes the results of the experiments conducted on the mock-up precast concrete sample to validate the performance of the proposed quality assurance system.

Overall dimensions check

Results calculated from the ICP and M3C2 algorithms described earlier are visualized in **Fig. 8**, where the various colors indicate the magnitude of M3C2 distances on each point, representing the deviations between the design and the real product. In this precast concrete sample, the upper-left corner exceeds the tolerance because of over-etching or excessive sandblasting and the conjunction lines between different surface finishes also have significant differences due to the molding inaccuracy. The proposed quality system can check both overall dimension quality and irregular shapes in the real product.

Embedded parts location check

The results of the embedded parts location check are visualized in **Fig. 9**, in which the blue boxes represent the design metal plate locations while the yellow boxes represent the measurements. The error is annotated by the side of each metal plate, where green represents an acceptable difference and red represents an unacceptable difference. The tolerance to distinguish the acceptance is currently set to 0.1 inches and can be modified given production requirements. In general, the mismatching of the two colored boxes indicates the direction of the error, and the calculated annotated error number indicates numerically how much the difference is.

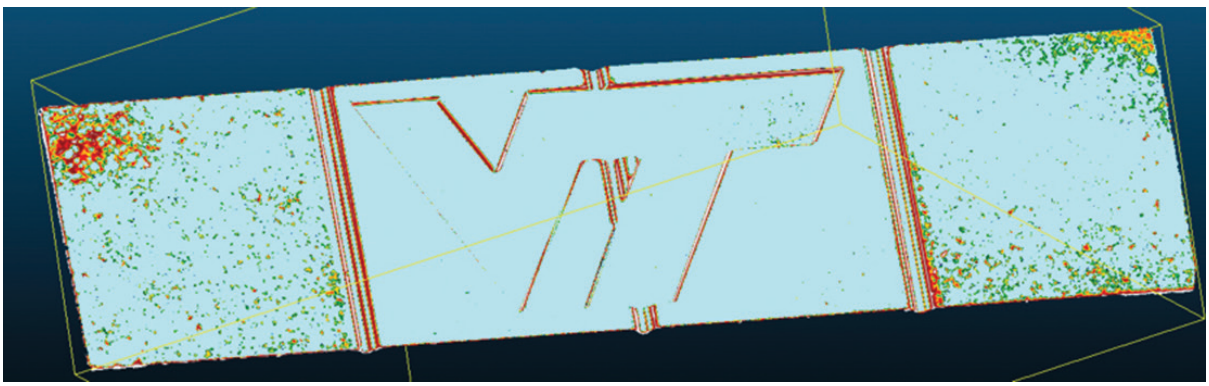

Figure 8. Geometry comparison between the scanned surface and the computer-aided design. The difference is following the cyan-green-yellow-red order, where red means the area with the largest deviations.

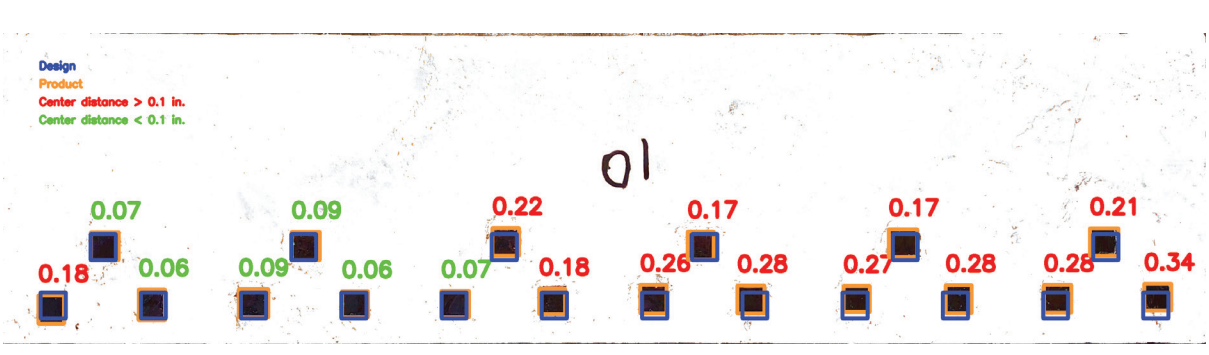

Figure 9. Results of back metal detection and comparison, where green indicates acceptable and red means out of range. Note: 1 in. = 25.4 mm.

Surface finish check

Table 1 presents the quantified results of the surface finish check for the sample's five different surface finishes. The results show substantial differences in mean values among the different surface finishes. The mean values can be used to automatically differentiate and recognize the type of surface finish during the quality inspection. The control limit is set to 1 standard deviation from the mean. It can provide a quantitative guideline for workers to perform sandblasting. The first two rows in **Fig. 10** illustrate graphical tools—a histogram of absolute distances and 3-D visualization of different surface finishes—that can be used to visualize the differences among various surface finishes. The last row in Fig. 10 shows the calculated roughness at selected subregions. This graph can be accessed in the developed GUI, where the user can define the location and size of the subregions.

Table 1. Mean, standard deviation, and tolerance for each surface finish region

Type of surface finish	Mean	Standard deviation	Tolerance
Heavy	0.2759	0.0371	0.2759 ± 0.0371
Medium	0.2115	0.0215	0.2115 ± 0.0215
Retarded	0.1065	0.0099	0.1065 ± 0.0099
Light	0.0527	0.0078	0.0527 ± 0.0078
Brush	0.0245	0.0030	0.0245 ± 0.0030

Graphical user interface

The algorithms of the three quality control functions are integrated into a GUI, which was built in Python on the Tkinter library. The GUI contains four parts: a menu (for loading all the necessary data) and the three quality inspection modules (**Fig. 11**).

Module 1: Metal plate location

Figure 12 illustrates the process and results of module 1. The inputs required to activate module 1 are an image (PNG or JPEG) of the back of the precast concrete part and a comma-separated value (CSV) file with design positions of metal plate and dimensions of the precast concrete sample.

Module 2: Overall dimension check

As described earlier, the process of overall dimension check includes three steps:

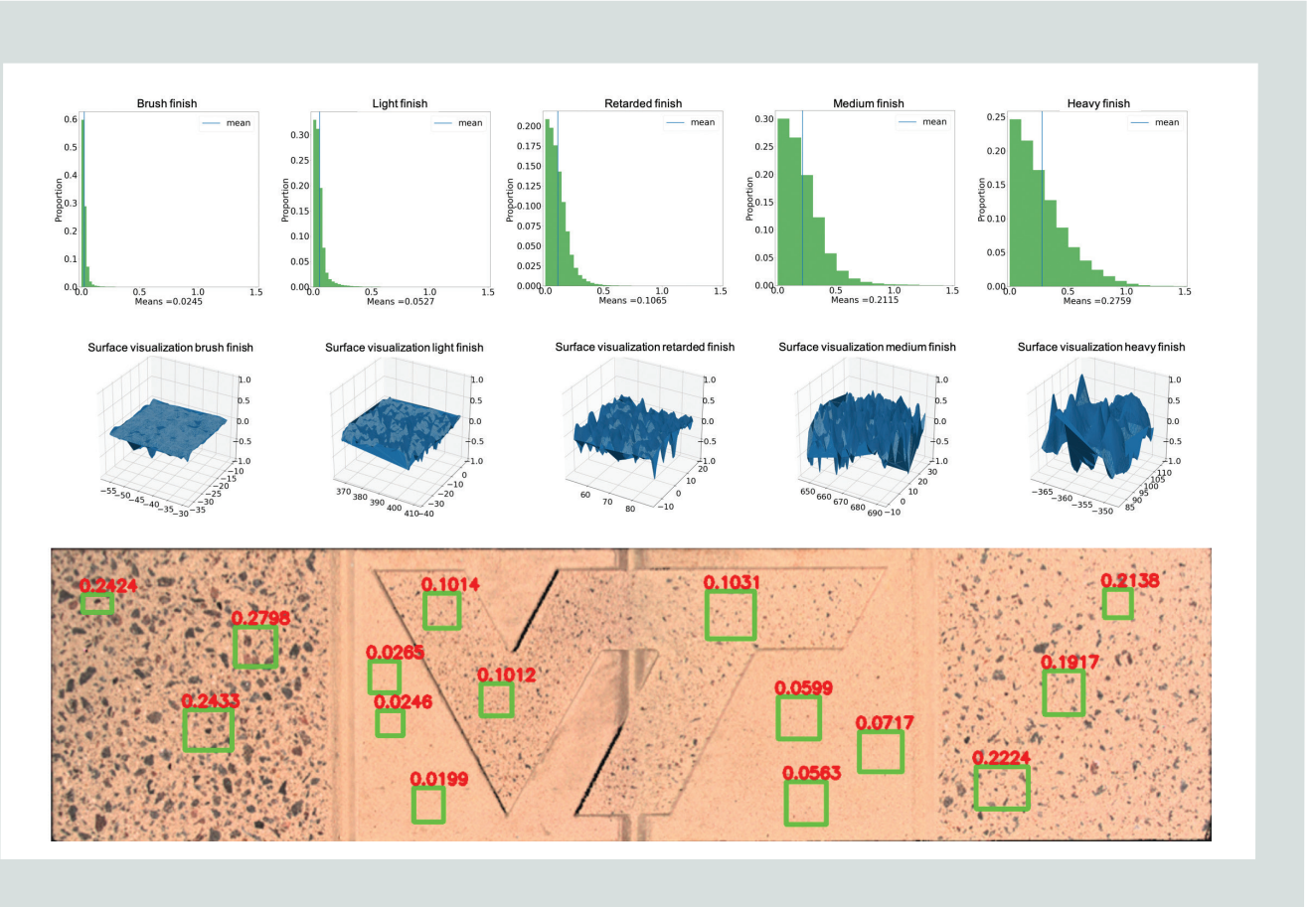

Figure 10. The top row shows the surface finish quantification results for brush, light, retarded, medium, and heavy finishes. The second row shows the surface finish visualization (examples) for brush, light, retarded, medium, and heavy finishes. The third row shows quantified surface roughness on example regions.

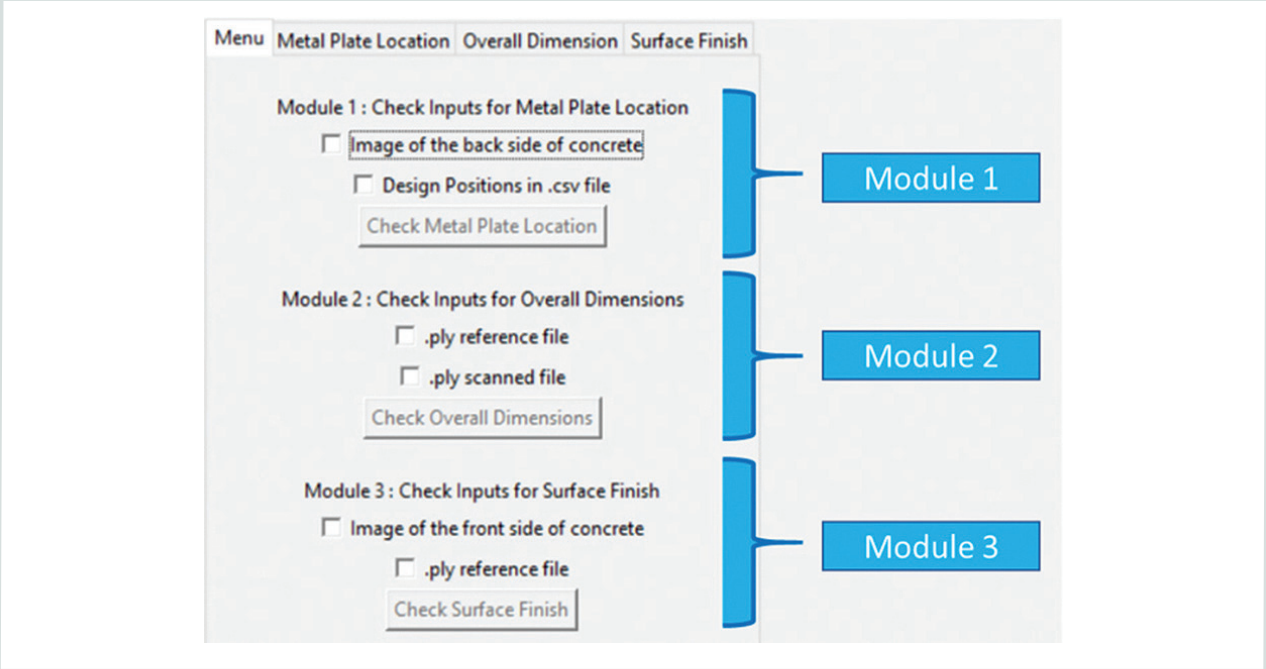

Figure 11. Menu tab on the graphical user interface along with the three module tabs.

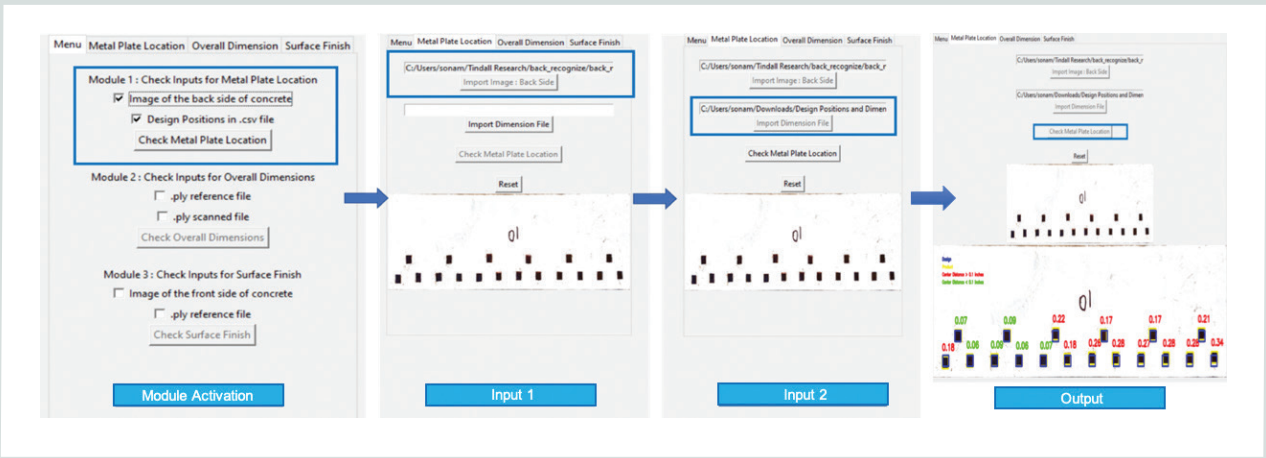

Figure 12. Process and result of module 1: metal plate location.

1. Register the ICP between the designed point cloud from the CAD model and scanned point cloud data.
2. Calculate the pointwise distance based on registration results.
3. Visualize the distance to show the difference between the designed product and the real product.

The following are the primary inputs required to activate the first step of module 2:

- the PLY reference file of the front side of the precast concrete part (from the designed CAD file)
- the PLY scanned file of the front side of the precast concrete part
- the BIN file created from the registration process
- the ASC distance file created from the comparison (keyword "M3C2" in the filename)

The final overall dimension check can be visualized in the GUI (**Fig. 13**).

Module 3: Surface finish

The inputs required to activate module 3 are the .ply reference file of the front side of the precast concrete sample, the PNG or JPEG image of the front of the precast concrete sample, and the number of crop areas to be made. The crop area command activates the open 3-D window. **Figure 14** shows the cropping process and the evaluation results of cropped areas.

Summary and implementation suggestions

The proposed 3-D scanning-based precast concrete quality assurance system can quantitatively measure the surface finish of a precast concrete object, recognize and check the location of the embedded metal parts, and validate the overall geometry with the design. Additionally, the surface finish standard, developed based on the statistical analysis of different types of finishes, can be adapted for future surface quality inspection applications. The proposed quality assurance system can

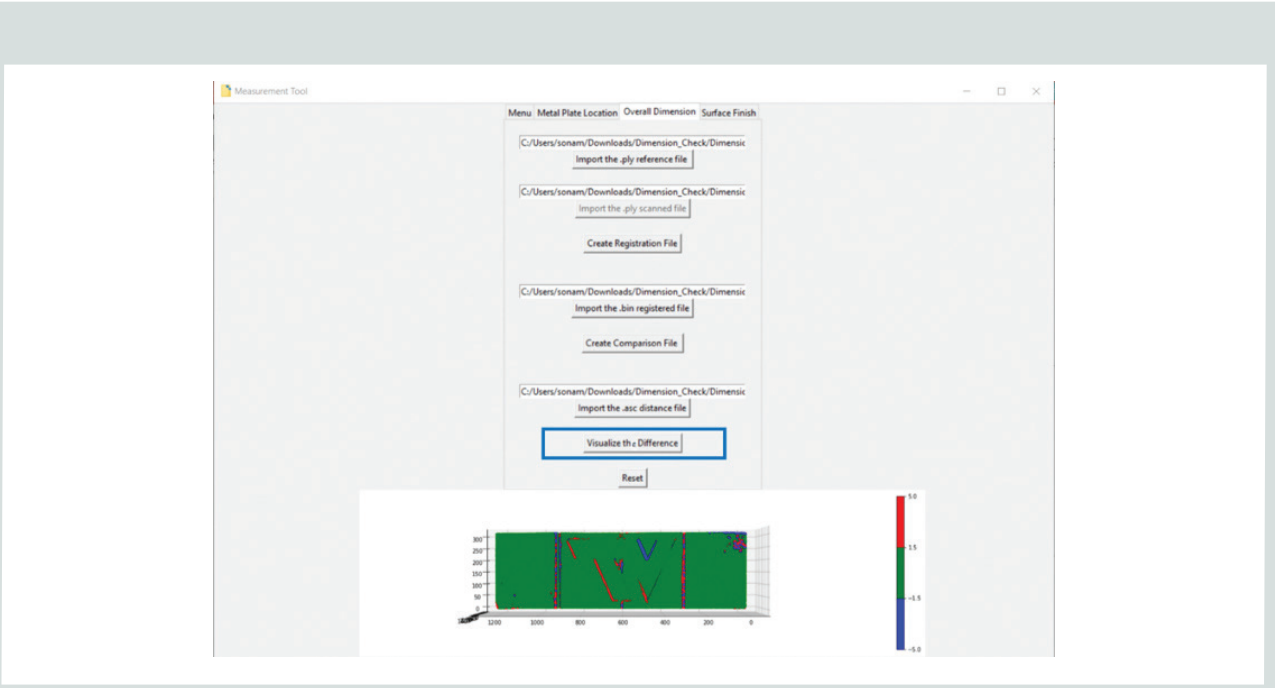

Figure 13. The final output of module 2: overall dimension check.

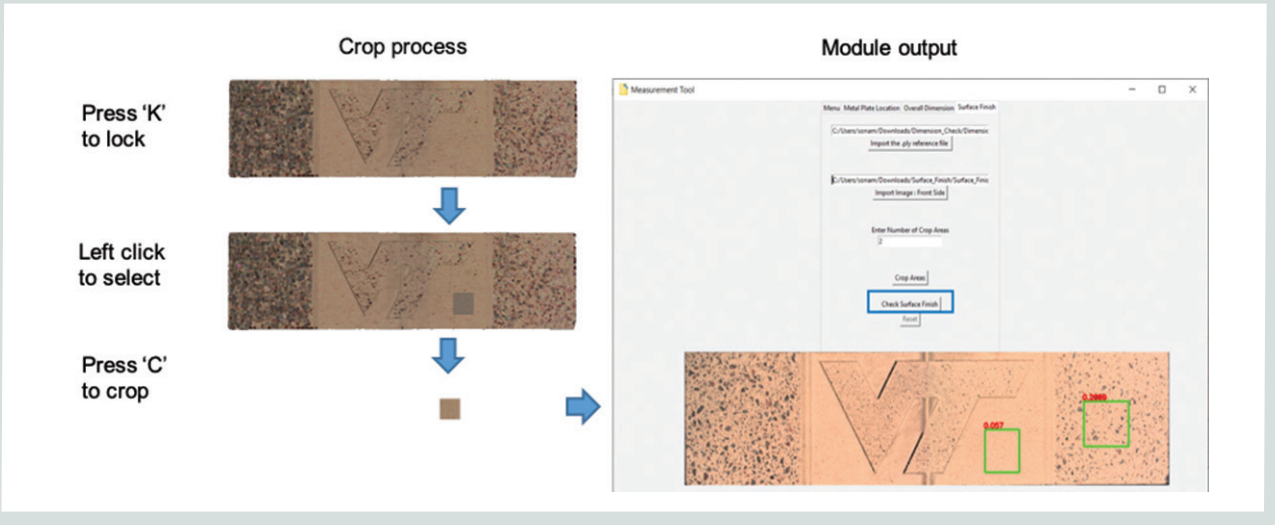

Figure 14. Crop process and output of module 3: surface finish.

provide high accuracy and efficient quality inspection and analysis. The scanned data and analysis results can be used for real-time analysis of product quality in the production process and the GUI software can satisfy the data analysis and visualization requirements in precast concrete quality inspection. Furthermore, this system can help to reduce operators' workload and safety hazards.

The system proved to be effective for the precast concrete quality assurance system and has the potential to be implemented in real practice.

For an industrial setup, a 3-D scanner with a larger field of view (FOV) than the currently marketed model must be built and calibrated. The long side of the FOV can be determined by the largest width of the products or the width of the crane. Most 3-D scanning software has stitching functions that can combine several scans to a whole part (the first two rows in Fig. 4). A 3-D scanner appropriate for industrial use can be built by modifying the currently available SLS system. Both the projector and the two cameras would need to be modified to fit the desired configuration.

In the factory, the entire scanning system could be mounted on a gantry crane with the projector on the center of the crane and the cameras at two sides, and faced downward. The suggested angle between the projector and camera is 15 ± 3 degrees.

A professional-grade projector (for example, Epson PowerLite L510U WUXGA 3LCD Laser Projector) would be needed to cover a large FOV with sufficient illumination. The lens of the original camera from the 3-D scanner has a zoom function that enables an adjustable FOV. If the coverage area were insufficient, replacing the lens with a shorter focal length would fix the problem.

Special cover cases might be required to protect the projector and cameras from the dusty industrial production environment. The cover cases could be made from acrylic sheets with integrated air filtering functions.

Before using the system, a calibration process would be needed to determine the relative angle and position between two cameras. The 3-D scanner manufacturer can provide the targets as well as other calibration instructions. This process would only need to be done once, as long as the cameras were not reinstalled.

During scanning, the concrete would not need to be positioned precisely at the exact location every time. As long as the concrete segment was within the FOV of the scanner, the whole process would function as expected.

Depending on the size of the sample and the required data spatial resolution, a precast concrete segment might require multiple scans. For example, using an SLS with a 3000 × 4000 pixel camera to scan a 15 × 20 ft (1.4 × 1.9 m) area provides 0.06 in. (15.2 mm) spatial resolution (the area divided by the number of pixels). With such resolution, to scan an 80 ft (24 m) long precast concrete object, five scans would be needed (20 + 15 + 15 + 15 + 15 ft [6.1 + 4.6 + 4.6 + 4.6 + 4.6 m], where the 15 ft lengths include 5 ft [1.5 m] of overlap for scan result–stitching purposes). A well-trained engineer could scan one part and complete the entire inspection process for that part in less than 10 minutes. For large products, additional time might be required to reposition the scanner.

Acknowledgments

This work is supported by PCI via the Daniel P. Jenny Fellowship program. We appreciate the support from Tindall Corp., which made the concrete sample. We also appreciate the constructive suggestions from Roger Becker and the PCI Research and Development Industry Advisory Committee, including Lee Lawrence, chair; Nathan Krause; Nathan Brooks; and Jason Woodard.

References

1. Woo, H., E. Kang, S. Wang, and K. H. Lee. 2002. "A New Segmentation Method for Point Cloud Data." *International Journal of Machine Tools and Manufacture* 42 (2): 167–178. https://doi.org/10.1016/S0890-6955(01)00120-1.

2. Kim, M. K., H. Sohn, and C. C. Chang. 2014. "Automated Dimensional Quality Assessment of Precast Concrete Panels Using Terrestrial Laser Scanning." *Automation in Construction* 45: 163–177. https://doi.org/10.1016/j.autcon.2014.05.015.

3. Wang, Q., M. K. Kim, S. Yoon, J. C. P. Cheng, and H. Sohn 2016. "Automated Quality Assessment of Precast Concrete Elements with Geometry Irregularities Using Terrestrial Laser Scanning." *Automation in Construction* 68: 170–182. https://doi.org/10.1016/j.autcon.2016.03.014.

4. Kim, M. K., Q. Wang, J. W. Park, J. C. P. Cheng, H. Sohn, C. C. Chang. 2016. "Automated Dimensional Quality Assurance of Full-Scale Precast Concrete Elements Using Laser Scanning and BIM." *Automation in Construction* 72 (2): 102–114. https://doi.org/10.1016/j.autcon.2016.08.035.

5. Liu, Y. F., S. Cho, B. F. Spencer, J. S. Fan. 2016. "Concrete Crack Assessment Using Digital Image Processing and 3D Scene Reconstruction." *Journal of Computing in Civil Engineering* 30 (1). https://doi.org/10.1061/(ASCE)CP.1943-5487.0000446.

6. Kim, M. K., H. Sohn, and C. C. Chang. 2015. "Localization and Quantification of Concrete Spalling Defects Using Terrestrial Laser Scanning." *Journal of Computing in Civil Engineering* 29 (6). https://doi.org/10.1061/(ASCE)CP.1943-5487.0000415.

7. Wang, Q., M. K. Kim, H. Sohn, and J. C. P Cheng. 2016. "Surface Flatness and Distortion Inspection of Precast

Concrete Elements Using Laser Scanning Technology." *Smart Structures and Systems* 18 (3): 601–623. https://doi.org/10.12989/sss.2016.18.3.601.

8. Gonzalez-Aguilera, D., J. Gomez-Lahoz, and J. Sanchez. 2008. "A New Approach for Structural Monitoring of Large Dams with a Three-Dimensional Laser Scanner." *Sensors* 8 (9): 5866–5883. https://doi.org/10.3390/s8095866.

9. Riveiro, B., H. González-Jorge, M. Varela, D.V. Jauregui. 2013. "Validation of Terrestrial Laser Scanning and Photogrammetry Techniques for the Measurement of Vertical Underclearance and Beam Geometry in Structural Inspection of Bridges." *Measurement* 46 (1): 784–794. https://doi.org/10.1016/j.measurement.2012.09.018.

10. Oskouie, P., B. Becerik-Gerber, and L. Soibelman. 2016. "Automated Measurement of Highway Retaining Wall Displacements Using Terrestrial Laser Scanners." *Automation in Construction* 65: 86–101. https://doi.org/10.1016/j.autcon.2015.12.023.

11. Fröhlich, C., and M. Mettenleiter. 2004. "Terrestrial Laser Scanning—New Perspectives in 3D Surveying." *International Archives of Photogrammetry, Remote Sensing and Spatial Information Sciences*. 36 (8 W2): 7–13. https://www.isprs.org/proceedings/xxxvi/8-w2/FROEHLICH.pdf.

12. Mikhail, E. M., J. S. Bethel, and J. C. McGlone. 2001. *Introduction to Modern Photogrammetry*. New York: Wiley and Sons.

13. Geng, J. 2011. "Structured-Light 3D Surface Imaging: A Tutorial." *Advances in Optics and Photonics* 3 (2): 128–160. https://doi.org/10.1364/AOP.3.000128.

14. Zhang, Z. Y. 1994. "Iterative Point Matching for Registration of Free-Form Curves and Surfaces." *International Journal of Computer Vision* 13 (2): 119–152. https://doi.org/10.1007/BF01427149.

15. Lague, D., N. Brodu, and J. Leroux. 2013. "Accurate 3D Comparison of Complex Topography with Terrestrial Laser Scanner: Application to the Rangitikei Canyon (N-Z)." *ISPRS Journal of Photogrammetry and Remote Sensing* 82: 10–26. https://doi.org/10.1016/j.isprsjprs.2013.04.009.

16. Suzuki, S., and K. Abe. 1985. "Topological Structural-Analysis of Digitized Binary Images by Border Following." *Computer Vision Graphics and Image Processing* 30 (1): 32–46. https://doi.org/10.1016/0734-189X(85)90016-7.

Notation

A = spatial coordinate

b = vector

B = height coordinate

C = designed point cloud

D = distance between point cloud and fitted plane

$dist(.)$ = distance function evaluating the difference between two point clouds

H = height of the image (both grayscale and color)

I = RGB image

$\tilde{I}$ = the grayscale image with the shape of $H \times W$

$I_{i,j}(1)$ = the intensity of color red

$I_{i,j}(2)$ = the intensity of color green

$I_{i,j}(3)$ = the intensity of color blue

$\tilde{I}_{i,j}$ = the grayscale pixel intensity at position (i,j) in grayscale image

$\tilde{I}_{i-1,j}$ = the intensity of pixel at position $(i-1,j)$ in grayscale image $\tilde{I} \in \mathbb{R}^{H \times W}$

$\tilde{I}_{i+1,j}$ = the intensity of pixel at position $(i+1,j)$ in grayscale image $\tilde{I} \in \mathbb{R}^{H \times W}$

$\tilde{I}_{i,j-1}$ = the intensity of pixel at position $(i,j-1)$ in grayscale image $\tilde{I} \in \mathbb{R}^{H \times W}$

$\tilde{I}_{i+1,j}$ = the intensity of pixel at position $(i,j+1))$ in grayscale image $\tilde{I} \in \mathbb{R}^{H \times W}$

R = rotation matrix

S = scanned point cloud

$\tilde{S}$ = registered scanned point cloud

T = translation matrix

W = width of the image (both grayscale and color)

(x, y) = coordinate of designed center point of metal plates

$(\hat{x}, \hat{y})$ = coordinate of measured center position of metal plates in product

(x_i, y_i, z_i) = coordinate of a single point in the point cloud

β = unknown parameters of the fitted plane

$\hat{\beta}$ = estimated parameters of the fitted plane

About the authors

Rongxuan Wang is a PhD student at the Grado Department of Industrial and Systems Engineering at the Virginia Polytechnic Institute and State University in Blacksburg, Va., specializing in sensing techniques such as three-dimensional scanning, digital image correlation, radiology, and thermography. His research focuses on process monitoring and quality control in smart manufacturing.

Yinan Wang is a PhD student at the Grado Department of Industrial and Systems Engineering at the Virginia Polytechnic Institute and State University. His research interests include data analytics, system pattern recognition, machine learning techniques in material/system design, and advanced manufacturing.

Sonam Devadiga is a master of science student at the Grado Department of Industrial and Systems Engineering at the Virginia Polytechnic Institute and State University.

Issac Perkins is plant manager at Tindall Corp. in Petersburg, Va. His expertise includes operations management, construction management, process improvement, and lean manufacturing.

Zhenyu (James) Kong, PhD, is a professor at the Grado Department of Industrial and Systems Engineering at the Virginia Polytechnic Institute and State University and a fellow of the Institute of Industrial and Systems Engineers (IISE). His research focuses on sensing and analytics for smart manufacturing. Kong is an associate editor for *IEEE Transactions on Automation Science and Engineering* and *IISE Transactions*.

Xiaowei Yue is an assistant professor at the Grado Department of Industrial and Systems Engineering at the Virginia Polytechnic Institute and State University. His research focuses on machine learning and data analytics for advanced manufacturing. Yue is a U.S. Department of Defense Manufacturing Engineering Education Program faculty fellow and an associate editor for *IISE Transactions* and the *Journal of Intelligent Manufacturing*.

Rongxuan Wang and Yinan Wang contributed equally to this paper.

The corresponding author is Xiaowei Yue (xwy@vt.edu).

Abstract

Quality control is a crucial step in the fabrication of precast concrete products. There are three critical quality features: the fabrication consistency of surface finish, the dimensional accuracy of the overall geometry, and the positioning accuracy of the embedded parts. Existing quality control methods rely on tape measures and inspectors' experience, which may lead to measurement inconsistency, operator faults, and safety hazards. This paper proposes an innovative real-time quality inspection system for the three critical quality features. The system first uses a structured-light three-dimensional scanner to capture the surface and geometric data from the precast concrete parts and then calculates and visualizes the deviations by applying specially developed algorithms. In addition, all of the functions are compiled into a graphical user interface that can be easily used by operators without a data analytics background. The system has been tested on a precast concrete sample with five different surface finishes in five regions of the sample, complex geometries, and a variety of embedded parts. The experiment results show that the proposed quality inspection and data analysis system can obtain critical quality information efficiently and accurately.

https://doi.org/10.15554/pcij66.6-01

Keywords

Computer-aided design, dimension check, embedded part, machine vision, point cloud data, quality assurance, structured-light scanning three-dimensional scanner, surface quality.

Review policy

This paper was reviewed in accordance with the Precast/Prestressed Concrete Institute's peer-review process.

Reader comments

Please address any reader comments to *PCI Journal* editor-in-chief Tom Klemens at tklemens@pci.org or Precast/Prestressed Concrete Institute, c/o PCI Journal, 8770 W. Bryn Mawr Ave., Suite 1150, Chicago, IL 60631.